IoT Enabled UAV: Network Architecture and Routing Algorithm

Qixun Zhang, *Member, IEEE*, Menglei Jiang, *Student Member, IEEE*, Zhiyong Feng, *Senior Member, IEEE*, Wei Li, *Senior Member, IEEE*, Wei Zhang, *Fellow, IEEE*, and Miao Pan, *Senior Member, IEEE*

***Abstract*—Unmanned aerial vehicles (UAVs) can be deployed efficiently to provide high quality of service for Internet of Things (IoT). By using cooperative communication and relay technologies, a large swarm of UAVs can enlarge the effective coverage area of IoT services via multiple relay nodes. However, the low latency service requirement and the dynamic topology of UAV network bring in new challenges for the effective routing optimization among UAVs. In this paper, a layered UAV swarm network architecture is proposed and an optimal number of UAVs is analyzed. Furthermore, a low latency routing algorithm (LLRA) is designed based on the partial location information and the connectivity of the network architecture. Finally, the performance of the proposed LLRA is verified by numerical results, which can decrease the link average delay and improve the packet delivery ratio in contrast to traditional routing algorithms without layered architecture.**

***Index Terms*—Internet of Things (IoT), network architecture, routing optimization, unmanned aerial vehicle (UAV).**

I. Introduction

AS AN emerging technology, unmanned aerial vehicles (UAVs) or drones have attracted much attention for critical important applications in border surveillance, environmental monitoring, disaster surveillance, and aerial photography [1]. Compared to conventional manned vehicles, UAVs can be configured by software programs via a remote controller, which are suitable for emergence and dangerous missions without personnel involved. Moreover, a swarm of UAVs can work cooperatively to accomplish complex tasks in a large area, such as the survivor search and rescue [2], which is one of the promising UAV enabled applications in the future.

In terms of the increasing demand for a guaranteed quality of service (QoS), traditional cellular network planning technology is time-consuming and lack of flexibility in both coverage extension and capacity improvement. With the accessibility to faraway rural areas and the quick response to emergency communication requirements, UAVs have the capability to assist land mobile systems to achieve a good coverage and offload the heavy data traffic [3], [4]. UAV can assist BSs to offload the data traffic, due to its high mobility and flexibility. Moreover, the trajectory of UAV at the edges of three adjacent cells is studied to offload traffic for BSs to support the rapidly increasing data services for cell-edge users [5]. Moreover, UAV can be used to assist the secure transmission for scalable videos in hyper-dense networks via caching, and the UAVs equipped with caches to store videos at off-peak time can act as SBSs to provide videos to mobile users in some small cells, which can reduce the pressure of wireless backhaul [6].

Furthermore, a swarm of UAVs can communicate with each other cooperatively via relay nodes to build a self-organized intelligent UAV network to accomplish complex tasks. According to the latest investigation of Federal Aviation Administration in [7], about seven million drones are expected to operate in the U.S. by 2020, which will propose challenges for the management and control of UAVs, especially for a large swarm and various types of UAVs. Considering different size, coverage range, and flying capability for various types of UAVs, the large size UAVs with longer endurance flight time and better communication capabilities can carry long-term periodic movements at high altitude to patrol and monitor a wide area, while the small size UAV with more flexible flight capabilities can be deployed in formation to work cooperatively at low altitude to collect and transmit sensing information or act as relay station to assist the communication among users on the ground. Therefore, different types of UAVs can work cooperatively to form a large layered network to carry out the tasks of disaster patrol and wide area environmental monitoring efficiently. In the layered UAV network, the large size UAVs flight at high altitude acting as upper layer UAVs, while the small size UAVs flight at low altitude acting as lower layer UAVs. And upper layer UAVs can act as

Manuscript received September 2, 2018; revised November 17, 2018; accepted December 22, 2018. Date of publication January 1, 2019; date of current version May 8, 2019. The work of Q. Zhang, M. Jiang, and Z. Feng was supported in part by the National Science and Technology Major Project under Grant 2017ZX03001014, in part by the National Natural Science Foundation of China under Grant 61790553 and Grant 61525101, in part by the China Scholarship Council under Grant 201806475028, and in part by the 111 Project of China under Grant B16006. The work of W. Zhang was supported in part by the National Natural Science Foundation of China under Grant 61728105 and in part by the Australian Research Council under Project DP160104903 and Project LP160100672. The work of M. Pan was supported in part by the U.S. National Science Foundation under Grant CNS-1343361, Grant CNS-1350230 (CAREER), Grant CNS-1646607, Grant CNS-1702850, and Grant CNS-1801925. *(Corresponding author: Zhiyong Feng.)*

Q. Zhang, M. Jiang, and Z. Feng are with the Key Laboratory of Universal Wireless Communications, Ministry of Education, School of Information and Communication Engineering, Beijing University of Posts and Telecommunications, Beijing 100876, China (e-mail: zhangqixun@bupt.edu.cn; jiangmenglei@bupt.edu.cn; fengzy@bupt.edu.cn).

W. Li is with the Department of Electrical Engineering, Northern Illinois University, DeKalb, IL 60115 USA (e-mail: weili@ieee.org).

W. Zhang is with the School of Electrical Engineering and Telecommunications, University of New South Wales, Sydney, NSW 2052, Australia (e-mail: w.zhang@unsw.edu.au).

M. Pan is with the Department of Electrical and Computer Engineering, University of Houston, Houston, TX 77204 USA (e-mail: mpan2@uh.edu).

Digital Object Identifier 10.1109/JIOT.2018.2890428

the central node to assist data transmission among lower layer UAVs.

Besides, UAVs are foreseen as an important component of the advanced cyber-physical Internet of Things (IoT) ecosystem [8]. IoT aims at enabling things to be connected anytime, anywhere ideally using any network and providing any service. Due to the fact that UAVs have many unique characteristics, such as the easy deployment, the reprogrammable ability during run-time, and the autonomous fly ability, UAVs have become an integral part of IoT infrastructure [8]. Moreover, UAVs can be deployed flexibly to set up an aerial subnetwork, which can collect and transmit the sensing data of unknown areas [9]. Equipped with IoT sensing devices (e.g., imaging sensors, position sensors, cameras, etc.) UAVs can collect data from different IoT devices, process the collected data, and deliver the data to the processing center [8]. Therefore, UAV technology can be fully utilized to support IoT services, such as the surveillance for earthquake and forest fire disasters, which are dangerous for people to enter. However, many challenges need to be addressed in order to achieve these goals.

For example, in a forest fire scenario, a swarm of UAVs equipped with different sensors need to be deployed efficiently to establish an emergency communication system, collecting different types of data (such as temperature, pressure, video, etc.) in Fig. 1. Due to the transmit power limit of equipments in UAVs, it is necessary to design a reliable and efficient UAVs relay network to guarantee a good coverage for the monitoring data collection in a large area. Especially, considering the low latency demand for the disaster rescue scenario, the efficient information collection is crucial for a swarm of UAVs from various data collecting devices to the data processing center. Moreover, the dynamic characteristics of UAVs network also bring new challenges to the stability of data transmission. Therefore, in order to establish an efficient UAV-assisted emergency communication system, there are many challenging problems unsolved, such as the network architecture design for an efficient cooperative communication among UAVs, and the low latency routing algorithm (LLRA) with dynamic network topology constraints.

In this paper, a layered UAV network architecture is proposed and the optimal number of UAVs in the upper layer is analyzed theoretically with closed-form coverage boundaries. Furthermore, based on the proposed network architecture, an LLRA is designed by using partial information of the location and network connectivity of UAVs. Based on the minimum delay and the estimated link stability of UAVs, the proposed LLRA can achieve the optimal route with the minimum delay and dynamically distribute various types of data traffic flows, which can efficiently maximize the packet delivery ratio and improve the stability of route.

A. Related Works

This paper has proposed a layered UAV network architecture, where different types of UAVs can be divided into various task layers and cooperate with each other. Besides, based on the proposed layered network architecture, the proposed LLRA algorithm has been designed to minimize the time delay and maximize the packet delivery ratio. And the related research works are briefly summarized in two aspects below.

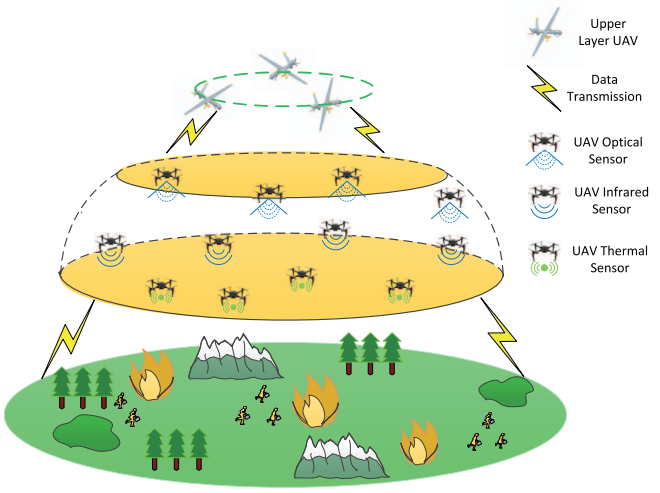

Fig. 1. Typical layered UAV network scenario for forest fire prevention and inspection.

1) Network Architecture of Layered UAVs: In terms of the demand for network coverage recovery in an emergency communication scenario, UAVs can be deployed efficiently to provide high QoS for mobile users. To investigate the effective coverage of UAV's deployment, an optimal altitude for a single static UAV is derived with the maximum coverage range [10]. Furthermore, an energy-efficient 3-D placement of UAV base station is studied [11], which can maximize the number of serving users within its coverage by decoupling the UAV base station placement problem into both vertical and horizontal dimensions. However, these research works neither consider about multiple UAVs nor the mobility effect to the coverage optimization problem of multiple UAVs. Besides, the impact of altitude on the minimum required transmit power is studied in the scenario with two UAVs [12]. The cooperative coverage enhancement scheme is further proposed in [13] for two UAVs, which are deployed over a geographic area with mobile users. However, these works only consider about two UAVs and ignore the impact of users' distributions on the performance of UAVs network. A novel approach for optimally deploying UAV base stations is proposed in [14] to provide a high data rate service to ground users while minimizing the overall UAV transmit power. The optimal cell boundaries and locations of UAVs are derived in the downlink scenario for multiple UAVs, which can minimize the required transmit power. But, this research work only considers about UAVs with the same flying capability and task demand, which omits the practical scenario with different flying abilities UAVs performing various tasks. Therefore, in terms of different types of UAVs with various capabilities, how to design a coverage optimized UAV network is a new challenging problem.

2) Low Latency Routing Algorithm of UAVs: Considering the high mobility of UAV in a 3-D space, traditional routing algorithms for mobile ad-hoc networks (MANETs) and

vehicle networks in 2-D are no longer appropriate for the UAV network scenario [15]. Existing routing protocols in MANETs and VANETs cannot be directly applied in UAVs, which should consider about the high mobility of UAVs, drastically changing network topology, and intermittently connected communication links in [16]. In contrast, the topology of UAVs changes more frequently, leading to the reliable connectivity among UAVs a challenging problem. In the literature, some research works have been done on the routing protocol for UAV networks. In the load-carry-and-deliver (LCAD) routing algorithm [17], the flying UAVs are used to deliver data packets from source to destination. Compared to conventional multihop store-and-forward routing protocols, LCAD provides a much higher network throughput. However, due to the coverage limit of single UAV, LCAD can only be used in a delay-tolerant network, and the packet delivery latency will increase linearly with the increase of distance between source and destination. Thus, a mobility and load aware optimized link-state routing (ML-OLSR) protocol is designed by using the mobility-aware and load-aware information [18]. Furthermore, traditional optimized link-state routing (OLSR) protocol is upgraded into a predictive-OLSR protocol by considering the effect of neighbor node's speed on the expected transmission count metric [19]. However, these protocols ignore the impact of UAV topology on the routing algorithm. Furthermore, ad hoc on-demand distance vector (AODV) performs well in a dynamic link condition with a low processing and memory overhead [20]. But, the delay of AODV routing algorithm is a big issue during the initial route discovery process. In addition, the link failure may trigger a route discovery, leading to both the extra latency and bandwidth occupation with the increase of network scale. As a consequence, the system throughput will drop dramatically as intermittent links become more pervasive. Based on AODV, a reactive-greedy-reactive protocol [21] was proposed for UAVs, where the route with the fewest hops is preferred. Due to the high speed of UAVs, the static routing table within a proactive routing protocol, such as OLSR, is not effective for a dynamic network scenario. At the same time, in a reactive routing protocol, such as AODV, the repeat of routing establishment is time consuming before each packet transmission process. To solve these problems, researchers proposed a new kind of routing protocol based on the geographic location information [16], such as the greedy perimeter stateless routing, which can achieve the good performance on latency and throughput [22]. However, GPSR is not appropriate for a sparse routing environment. In addition, GPSR relies on a greedy forwarding algorithm and it may fail when a packet arrives at a node that has no neighbor node nearby. Besides, it requires an accurate location information which is hard to achieve in a practical scenario. Although these existing works have studied the routing problem and different routing algorithms are proposed, the latency of these routing algorithms increases tremendously with the increase of UAV network scale. Even worse, the network connectivity will be deteriorated due to the delay, interference, and dynamic topology variations in terms of a large swarm of UAVs.

B. Contributions

Therefore, to minimize the latency and guarantee the connectivity of UAVs for IoT services, this paper has proposed a layered UAV network architecture and an efficient routing algorithm is also designed to minimize the latency and maximize the packet delivery ratio. The contributions are summarized in two folds.

1) Compared to existing research works with multiple UAVs, the optimal number of UAVs based on the proposed layered network architecture is investigated by three typical cases in terms of the geometrical relation among different UAVs. The closed-form coverage boundaries of upper layer UAVs are achieved theoretically based on the proposed equivalent coverage model in this paper.
2) Based on the proposed layered network architecture, the LLRA algorithm has been designed by using partial information of the location and network connectivity of UAVs. Based on the estimated link stability of UAVs, LLRA algorithm can dynamically distribute different data traffic flows via the optimal relay notes, which can efficiently minimize the latency.

The rest of this paper is organized as follows. A layered UAV network architecture is proposed as the system model for the low latency routing problem formation in UAV enabled IoT scenario in Section II. To minimize the transmission latency for a large swarm of UAVs, the fundamental problem of the proposed layered architecture design is solved theoretically by closed-form coverage boundaries in two cases in Section III. Furthermore, the low latency routing optimization scheme is designed by taking into account both the location and connectivity of UAVs in Section IV. Numerical results are discussed in terms of the link average delay and the packet delivery ratio in Section V. Finally, Section VI concludes this paper.

II. System Model and Problem Formulation

UAVs can be deployed efficiently to provide the high QoS for IoT. By using cooperative communication and relay technologies, a large swarm of UAVs can enlarge the effective coverage area of IoT services via multiple relay nodes. Therefore, UAVs can be used to guarantee the communication performance during an emergency communication scenario of earthquake or forest fire, and UAV-based communication network can be utilized to collect information from various sensors, transmit real-time video stream, as well as support the robust information sharing among fire-fighters on the ground. However, the low latency service requirement for emergency information sharing among UAVs and the dynamic UAV network topology bring in new challenges to UAV network performance and effective routing optimization among UAVs.

To address these issues, both the layered UAV swarm network architecture and the LLRA are proposed to monitor the forest fire and ensure the performance of information sharing among UAVs in this paper. Different types of UAVs are divided into two layers according to various tasks, including the upper and lower layers, as shown in Fig. 1. Considering the diversity of coverage and flying capability of speed among

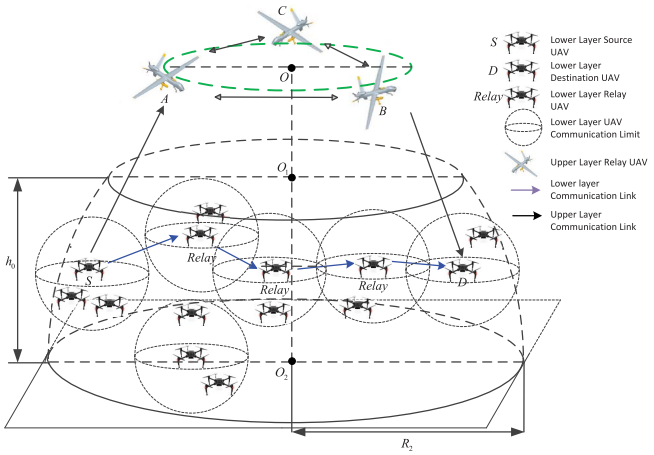

Fig. 2. Layered UAV network architecture.

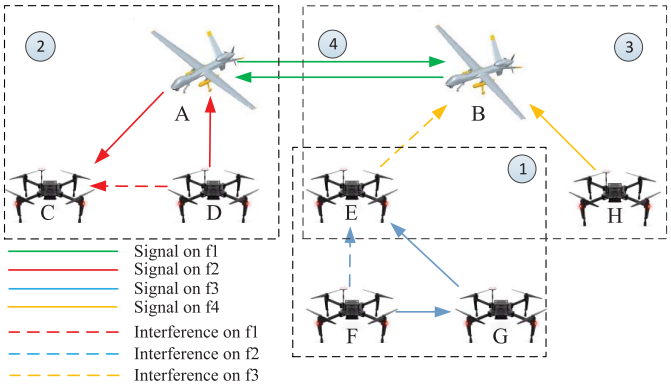

Fig. 3. Interference model for UAV network.

UAVs, the upper layer consists of fixed wing UAVs circulating in a circle, which can provide an effective coverage to UAVs in the lower layer by using directional antennas. Upper layer UAVs can act as relay nodes to assist the communication of lower layer UAVs and reduce the transmission delay.

Lower layer UAVs equipped with different sensors are responsible for collecting and transmitting the sensing data in an exploration area. Different kinds of sensor equipments can be utilized in various UAV platforms. Moreover, due to the transmission distance limit of various sensors, the lower layer UAVs are distributed at different heights according to various task requirements. Due to the large coverage requirement for forest fire monitoring, a swarm of UAVs is needed to be deployed in the lower layer. In order to verify the occurrence probability of forest fire and predict the speed of fire spread timely, the efficiency of information sharing among UAVs in the lower layer is crucial. Therefore, the low latency communication among lower layer UAVs is crucial. Therefore, the LLRA algorithm is designed based on the partial location and connectivity information of UAVs to improve the routing performance.

To simplify the analyses, the center of lower layer area is defined by O_2 with a radius of R_2. The lower layer area can be depicted by $V(x, y, z) = \{(x, y, z) : x^2 + y^2 + z^2 \leq {R_2}^2, z \leq h_0\}$, where h_0 represents the maximum flying height of lower layer UAVs as shown in Fig. 2. To guarantee the connectivity among UAVs in the lower layer, the omnidirectional antenna is applied as an efficient method to improve the communication opportunity among UAVs. The path loss model for each link between two UAVs is assumed to follow a proportion of $d^{-\alpha}$, where d is the distance between UAVs and α is the mean path loss exponent. The power gain of small scale fading channel h_{ij} is distributed exponentially with a unit mean and the noise N_0 is the additive white Gaussian noise following a distribution of $N_0 \sim (0, N)$ in [7].

Furthermore, to guarantee the performance of different UAVs, the interference issue should be take into consideration extensively, especially for the scenario of a large number of UAVs. It is also assumed that the upper layer UAV will communicate with the lower layer UAV on different frequency bands to avoid mutual interferences, while the communication links among UAVs in the upper layer or in the lower layer will operate on different frequency bands. Thus, the interference model for the proposed layered UAV network architecture is shown in Fig. 3, including four typical scenarios.

As shown by scenario 1 in Fig. 3, the interference of UAV E comes from UAV F and G in lower layer using omnidirectional antennas. The received signal to interference and noise ratio (SINR) between UAV i and UAV j with a distance of d_{ij} is denoted by SINR_{ij} in (1), where $i, j \in \Phi x$, and Φx is the set of lower layer UAVs. When the upper layer UAV A using a directional antenna communicates with the lower layer UAV C as shown by scenario 2, the SINR between UAV i and UAV j is denoted in (1), where $i \in \Phi s, j \in \Phi x$, and Φs is the set of upper layer UAVs. When the lower layer UAV H communicates with the upper layer UAV B as described by scenario 3, the SINR between UAV i and UAV j is shown in (1), where $i \in \Phi x, j \in \Phi s$. Finally, when UAV A and UAV B in the upper layer communicate with each other in scenario 4, the SINR between UAV i and UAV j is depicted by (1), where $i, j \in \Phi s$. Moreover, P_{ij} represents the transmission power from UAV i to UAV j and g_m represents the transmission gain ratio of UAVs in the upper layer by $g_m = (P/S_0)/(P/S_d) = (S_d/S_0) = [(4\pi r^2)/(2\pi r^2(1 - \cos\theta))] = [2/(1 - \cos\theta)]$, where θ is the radiation angle of directional antenna, P is the transmission power of upper layer UAVs. To theoretically calculate the effective coverage area of each upper layer UAV, the omnidirectional antenna spherical corona's area is defined as an entire ball surface area by S_d, where S_0 is the spherical corona's area of the directional antenna in Fig. 4. In general, the received SINR between UAV i and UAV j at a distance of d_{ij} can be simplified by (2), when the interference from lower layer UAVs is $\sum_{p\in\Phi x, p\neq j} P_{pj} h_{pj} {d_{pj}}^{-\alpha} = U_I, j \in \Phi x$

$$\text{SINR}_{ij} = \begin{cases} \dfrac{P_{ij} h_{ij} {d_{ij}}^{-\alpha}}{N_0 + \sum\limits_{p\in\Phi x, p\neq i, p\neq j} P_{pj} h_{pj} {d_{pj}}^{-\alpha}}, & i, j \in \Phi x \\ \dfrac{P_{ij} h_{ij} {d_{ij}}^{-\alpha} g_m}{N_0 + \sum\limits_{p\in\Phi x, p\neq j} P_{pj} h_{pj} {d_{pj}}^{-\alpha}}, & i \in \Phi s, j \in \Phi x \\ \dfrac{P_{ij} h_{ij} {d_{ij}}^{-\alpha} g_m}{N_0 + \sum\limits_{p\in\Phi x, p\neq i} P_{pj} h_{pj} {d_{pj}}^{-\alpha} g_m}, & i \in \Phi x, j \in \Phi s \\ \dfrac{P_{ij} h_{ij} {d_{ij}}^{-\alpha} g_m^2}{N_0}, & i, j \in \Phi s \end{cases} \quad (1)$$

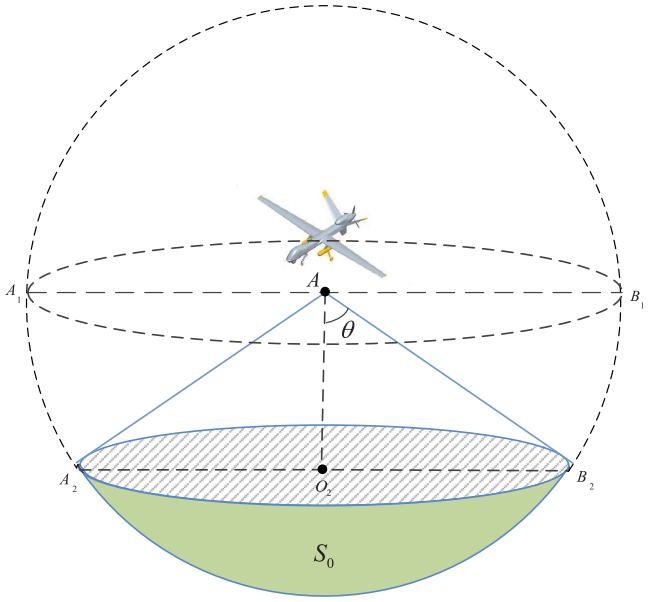

Fig. 4. Coverage model for upper layer UAV using directional antenna.

$$\mathrm{SINR}_{ij} = \begin{cases} \frac{P_{ij}h_{ij}d_{ij}^{-\alpha}}{N_0+U_I}, & i,j \in \Phi x \\ \frac{P_{ij}h_{ij}d_{ij}^{-\alpha}g_m}{N_0+U_I}, & i \in \Phi s, j \in \Phi x \\ \frac{P_{ij}h_{ij}d_{ij}^{-\alpha}g_m}{N_0+g_mU_I}, & i \in \Phi x, j \in \Phi s \\ \frac{P_{ij}h_{ij}d_{ij}^{-\alpha}g_m^2}{N_0}, & i,j \in \Phi s. \end{cases} \tag{2}$$

Based on (2), the successful packet transmission probability $P(\mathrm{SINR}_{ij} \geq \eta)$ is depicted by (3), where η is the SINR threshold. The mean interference at the center of lower layer is given by $U_I = [(3N(R_2^{3-\alpha} - \varepsilon^{3-\alpha}))/(2R_2^3(3-\alpha))]$ based on [26], where N is the total number of UAVs in a ball with a radius of R following a 3-D binomial point process distribution and ε is the minimum distance between lower layer UAVs. Theoretically, N is defined by $N = [(4\pi R_2^3 n)/(2\pi R_2^3 - \pi(R_2 - h_0)(2R_2^2 - h_0^2 - R_2 h_0))]$, where n is the number of lower layer UAVs

$$P\left(\mathrm{SINR}_{ij} \geq \eta\right) = \begin{cases} \exp\left(-\eta d_{ij}{}^{\alpha}\frac{N_0+U_I}{P_{ij}}\right), & i,j \in \Phi x \\ \exp\left(-\eta d_{ij}{}^{\alpha}\frac{N_0+U_I}{g_mP_{ij}}\right), & i \in \Phi s, j \in \Phi x \\ \exp\left(-\eta d_{ij}{}^{\alpha}\frac{N_0+g_mU_I}{g_mP_{ij}}\right), & i \in \Phi x, j \in \Phi s \\ \exp\left(-\eta d_{ij}{}^{\alpha}\frac{N_0}{g_m^2P_{ij}}\right), & i,j \in \Phi s. \end{cases} \tag{3}$$

To guarantee the QoS between UAV i and UAV j, $P(\mathrm{SINR}_{ij} \geq \eta) \geq \psi$ should be satisfied, where ψ is the QoS constraint of a successful transmission. Thus, the maximum effective distance $d_{ij\max}$ can be achieved in (4), when $P(\mathrm{SINR}_{ij} \geq \eta) = \psi$

$$d_{ij\max} = \begin{cases} \left(-\frac{P_{ij}\ln(\psi)}{\eta(N_0+U_I)}\right)^{\frac{1}{\alpha}}, & i,j \in \Phi x \\ \left(-\frac{g_mP_{ij}\ln(\psi)}{\eta(N_0+U_I)}\right)^{\frac{1}{\alpha}}, & i \in \Phi s, j \in \Phi x \\ \left(-\frac{g_mP_{ij}\ln(\psi)}{\eta(N_0+g_mU_I)}\right)^{\frac{1}{\alpha}}, & i \in \Phi x, j \in \Phi s \\ \left(-\frac{g_m^2P_{ij}\ln(\psi)}{\eta N_0}\right)^{\frac{1}{\alpha}}, & i,j \in \Phi s. \end{cases} \tag{4}$$

III. Coverage Optimization Design for Layered UAV Network

Considering the coverage limitation of each UAV in the upper layer constrained by the transmission power, several upper layer UAVs should cooperate with each other to guarantee an effective full coverage to lower layer UAVs. In order to minimize the communication latency and multiple relay hops in the proposed layered UAV network architecture, how to design the appropriate number of upper layer UAVs as relay nodes is a challenging coverage optimization problem. Therefore, the layered UAV network design problem is defined as how to deploy the minimum number of UAVs in the upper layer to realize an effective full coverage to lower layer UAVs. The coverage optimization scheme using the minimum number of upper layer UAVs is theoretically analyzed with closed-form coverage boundaries in two typical cases.

As shown in Fig. 5, the upper layer UAV A moves around the upper layer center O with a radius of D_{OA}. Based on the geometrical relation of D_{OA}, two typical situations are considered as shown in Fig. 5(a)–(d). When D_{OA} achieves its minimum, Fig. 5(a) and (b) depict the side view and the top view of the geometrical relation of upper layer UAV and its coverage area in the lower layer, respectively. Similarly, when D_{OA} achieves its maximum, Fig. 5(c) and (d) depict the side view and the top view of the geometrical relation of upper layer UAV and its coverage area in the lower layer. Moreover, the center points O, O_1, and O_2 in both upper and lower layers share the same position from the top view as depicted by Fig. 5(b) and (d). Upper layer UAVs have the same speed of V_A and $\angle JO_1K$ is the maximum angle of UAV's coverage by using the directional antenna. Based on (4), the maximum effective distance and coverage of scenario 2 are bigger than that of scenario 3 in Fig. 3. To guarantee the coverage requirements for both scenario 2 and 3 in Fig. 3, the coverage problem of scenario 2 is analyzed thereafter. To achieve an effective coverage in lower layer within T_0, the effective coverage time for UAVs is defined by t_0 in (5), where $\angle JO_1K$ is the maximum coverage angle in the tangent plane. Moreover, the radiation angle of directional antenna θ is less than the maximum angle of lower layer's tangent $\angle EO_2F$. Thus, the maximum angle of coverage $\angle JO_1K$ can be calculated by $\angle JO_1K = 2\arccos[(R_{O_1J}{}^2 - R_{A1}{}^2 + D_{O_1A_1}{}^2)/(2R_{O_1J}D_{O_1A_1})]$ in Fig. 5(c). Furthermore, R_{O_1J} is the radius of the cross section in lower layer at a height of h_{A1} and R_{A1} represents the radius of cross section of UAV's coverage in lower layer at a height of h_{A1}

$$t_0 = \frac{T_0\angle JO_1K}{2\pi} = \frac{T_0}{\pi}\arccos\frac{R_{O_1J}{}^2 - R_{A1}{}^2 + D_{O_1A_1}{}^2}{2R_{O_1J}D_{O_1A_1}}. \tag{5}$$

Furthermore, the relations among the radiation angle of directional antenna, the minimum number of upper layer UAVs, and the effective coverage time are analyzed in order to design a low latency routing scheme. It is also assumed that the minimum and maximum radiation angles of UAV A in the upper layer are depicted by $\theta_{\min}$ and $\theta_{\max}$, where $\theta_{\min} \leq \angle EO_2F \leq \theta_{\max}$. Since each upper layer UAV

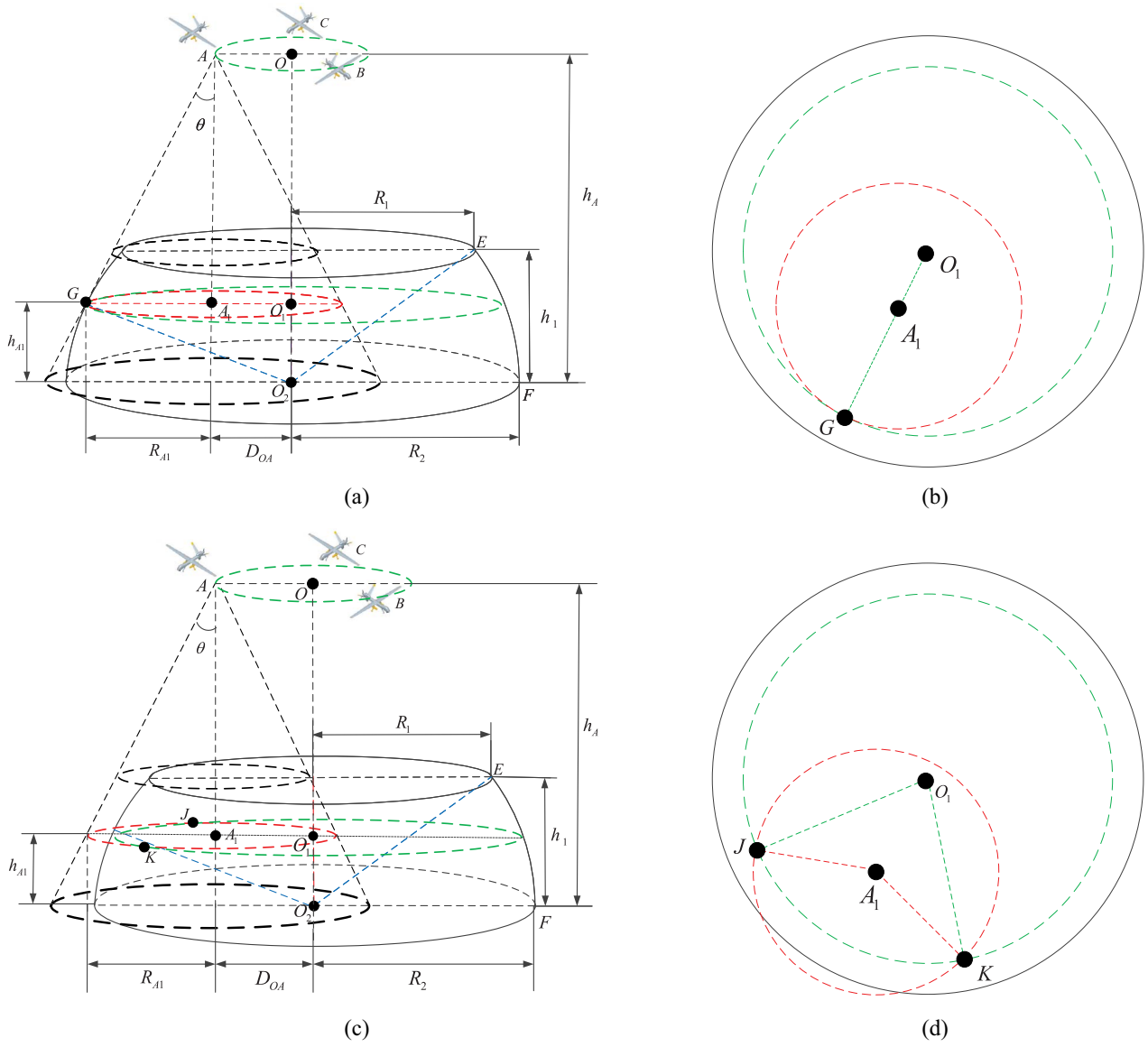

Fig. 5. Geometrical coverage model of upper layer UAVs for case 1. (a) D_{OA} is the minimum from side view. (b) D_{OA} is the minimum from top view. (c) D_{OA} is the maximum from side view. (d) D_{OA} is the maximum from top view.

cannot cover the whole area of a large number of lower layer UAVs, different upper layer UAVs should cooperate with each other to achieve an effective coverage in the lower layer. Thus, the minimum number problem of upper layer UAVs is converted to the effective coverage time maximization problem.

In order to maximum the effective coverage time of upper layer UAVs, two typical cases are considered based on whether the coverage boundary of upper layer UAVs can be tangent to the edge of lower layer area or not.

1) Case 1: When $\theta_{\min} \leq \theta \leq \angle EO_2F$, the coverage boundary of UAV A can be tangent to the edge of lower layer at G with a height of h_{A1}, where the radius D_{OA} achieved the minimum value as shown in Fig. 5(a). In Fig. 5(b) and (d), the black circle denotes the lower surface of lower layer area and the green dotted circle denotes the cross section of lower layer area with the height of h_{A1}, and the red dotted circle denotes the projection of the upper layer UAVs coverage area on green circle. Each upper UAV will have a projection of a red circle on the green circle, and only when the green circle is filled with red circles, upper layer UAVs can achieve the full coverage for the lower layer area. When D_{OA} changes, R_{O_1J} and R_{A1} are calculated in (6) based on their geometrical relations in Fig. 5, where R_2 is the radius of bottom lower layer

$$\begin{cases} R_{O_1J} = R_2 \cos\theta \\ R_{A1} = (h_A - R_2 \sin\theta)\tan\theta. \end{cases} \tag{6}$$

Based on (5) and (6), the effective coverage time t_0 can be calculated by (7). When D_{OA} and θ are constants, the effective coverage time t_0 will decrease as the value of h_A increases. However, the maximum altitude $h^{\theta}_{\max}$ of UAV A is constrained by its flight capability h_u and communication capability h_c. Thus, the maximum altitude $h^{\theta}_{\max}$ is

denoted by (8)

$$t_0 = \frac{T_0}{\pi} \arccos \times \frac{(R_2\cos\theta)^2 - [(h_A - R_2\sin\theta)\tan\theta]^2 + {D_{O_1A_1}}^2}{2R_2\cos\theta D_{O_1A_1}} \tag{7}$$

$$h^{\theta}_{\max} = \min(h_u, h_c) = \min\left(h_u, \cos\theta\left(-\frac{g_m P_{ij}\ln(\psi)}{\eta\left(N_0 + U_{Ig_m}\right)}\right)^{\frac{1}{\alpha}}\right). \tag{8}$$

As shown in Fig. 5, when the maximum altitude $h^{\theta}_{\max}$ and the radiation angle θ are constants, the range of D_{OA} is denoted by $D^{\theta}_{OA\min}$ and $D^{\theta}_{OA\max}$ in (9), where h_1 is the height of lower layer and $D^{\theta}_{OA\min} \le D_{OA} \le D^{\theta}_{OA\max}$, and $HL = (h^{\theta}_{\max} - R_2\sin\theta)\tan\theta$. Then, the maximum coverage time t^{θ}_0 and D^{θ}_{OA} are depicted in (10), where

$$f(D_{OA}) = \frac{T_0}{\pi}\arccos\frac{(R_2\cos\theta)^2 - \left[\left(h^{\theta}_{\max} - R_2\sin\theta\right)\tan\theta\right]^2 + {D_{O_1A_1}}^2}{2R_2\cos\theta D_{O_1A_1}}.$$

The ratio of the effective communication time of lower layer UAV to the total time of upper layer UAV is defined by the maximum effective coverage time ratio $t_{\max}$. Therefore, in case 1 when $\theta_{\min} \le \theta \le \angle EO_2F$, the maximum effective coverage time ratio $t_{\max 1}$ and the radiation angle θ_1 are achieved in (11)

$$\begin{cases} D^{\theta}_{OA\min} = R_{O_1J} - R_{A1} = R_2\cos\theta - HL \\ D^{\theta}_{OA\max} = \left(h^{\theta}_{\max} - h_1\right)\tan\theta \end{cases} \tag{9}$$

$$\begin{cases} D^{\theta}_{OA} = \min\left(D^{\theta}_{OA\ \max}, \sqrt{(R_2\cos\theta)^2 - HL^2}\right) \\ t^{\theta}_0 = f\left(D^{\theta}_{OA}\right) \end{cases} \tag{10}$$

$$\begin{cases} t_{\max 1} = \max\frac{t^{\theta}_0}{T_0} \\ \theta_1 = \arg\max\frac{t^{\theta}_0}{T_0}. \end{cases} \tag{11}$$

2) Case 2: When $\angle EO_2F < \theta \le \theta_{\max}$, the coverage boundary of UAV A cannot be tangent to the edge of lower layer. When the coverage boundary of UAV A intersects the edge of lower layer at G with a height of h_{A1}, where h_{A1} is the height of lower layer area, the radius D_{OA} achieved the minimum value as shown in Fig. 6(a). In Fig. 6(b) and (d), the black circle denotes the lower surface of lower layer area, the green dotted circle denotes the upper surface of lower layer area, and the red dotted circle denotes the projection of the coverage area of UAV A on green circle. Each upper UAV will have a projection of a red circle on the green circle, and only when the green circle is filled with red circles, upper layer UAVs can achieve the full coverage for the lower layer area.

When the radius D_{OA} changes, R_{O_1J} and R_{A1} are calculated in (12) based on the geometrical relation of UAVs. R_1 is the radius of top plane in the lower layer. Based on (5) and (12), the effective coverage time t_0 is calculated in (13)

$$\begin{cases} R_{O_1J} = R_1 \\ R_{A1} = (h_A - h_1)\tan\theta \end{cases} \tag{12}$$

$$t_0 = \frac{T_0}{\pi}\arccos\frac{{R_1}^2 - [(h_A - h_1)\tan\theta]^2 + {D_{O_1A_1}}^2}{2R_1 D_{O_1A_1}}. \tag{13}$$

When D_{OA} and θ are constants, the larger the value of h_A, the smaller the coverage time t_0 is base on (13). But, the maximum altitude $h^{\theta}_{\max}$ of UAV A is constrained by its flight capability h_u and communication capability h_c. When the maximum altitude $h^{\theta}_{\max}$ and the radiation angle θ are constants, the range of D_{OA} is denoted in (14) by $D^{\theta}_{OA\min}$ and $D^{\theta}_{OA\max}$. Because the range of D_{OA} is constrained by $D^{\theta}_{OA\min} \le D_{OA} \le D^{\theta}_{OA\max}$, the effective coverage time t^{θ}_0, and range D^{θ}_{OA} are calculated in (15), where

$$g(D_{OA}) = \left(\frac{T_0}{\pi}\right)\arccos\frac{{R_1}^2 - \left[\left(h^{\theta}_{\max} - h_1\right)\tan\theta\right]^2 + {D_{O_1A_1}}^2}{2R_1 D_{O_1A_1}}.$$

Therefore, in case 2 when $\angle EO_2F \le \theta \le \theta_{\max}$, the maximum effective coverage time ratio $t_{\max 2}$ and the radiation angle θ_2 are achieved in (16)

$$\begin{cases} D^{\theta}_{OA\min} = R_{O_1J} - R_{A1} = R_1 - \left(h^{\theta}_{\max} - h_1\right)\tan\theta \\ D^{\theta}_{OA\max} = \left(h^{\theta}_{\max} - h_1\right)\tan\theta \end{cases} \tag{14}$$

$$\begin{cases} D^{\theta}_{OA} = \min\left(D^{\theta}_{OA\ \max}, \sqrt{{R_1}^2 - \left[\left(h^{\theta}_{\max} - h_1\right)tan\theta\right]^2}\right) \\ t^{\theta}_0 = g\left(D^{\theta}_{OA}\right) \end{cases} \tag{15}$$

$$\begin{cases} t_{\max 2} = \max\frac{t^{\theta}_0}{T_0} \\ \theta_2 = \arg\max\frac{t^{\theta}_0}{T_0}. \end{cases} \tag{16}$$

In general, the optimal deployment location and the radiation angle of directional antenna of the upper layer UAV A are based on the maximum effective coverage time ratio $t_{\max}$, which is bounded between $t_{\max 1}$ and $t_{\max 2}$. And the radiation angle θ, altitude $h^{\theta}_{\max}$, and radius D^{θ}_{OA} can be calculated according to the theoretical analysis in two typical cases. Finally, the minimum number of upper layer UAVs is solved by $N_{\min} = [[1/(t_{\max})]]$. Therefore, the layered UAV network architecture can be designed with the minimum number of upper layer UAVs and the effective full coverage to lower layer UAVs based on coverage boundary results.

IV. Low Latency Routing Optimization Scheme

Based on the proposed layered UAV network architecture, both the minimum number of upper layer UAVs and the optimal deployment location and the radiation angle of directional antenna of the upper layer UAV have been achieved with theoretical analysis in Section III. Thereafter, the LLRA is designed based on the proposed layered UAV network architecture, and two cases are considered based on whether upper layer UAVs can realize an effective full coverage to lower layer UAVs or not.

In the first case, upper layer UAVs can realize the full coverage of lower layer UAVs, and all lower layer UAVs can communicate with at least one upper layer UAVs directly. Therefore, the lower layer UAVs can communicate with each other directly or through the upper layer UAV. In the second case, the number of upper layer UAVs is less than $N_{\min}$, and upper layer UAVs cannot realize the full coverage of lower layer UAVs, which will result in the coverage blind zone in the lower layer with analysis proposed in Section IV-A. Lower layer UAVs in the coverage blind zone cannot communicate with upper layer UAVs directly, so an efficient routing is

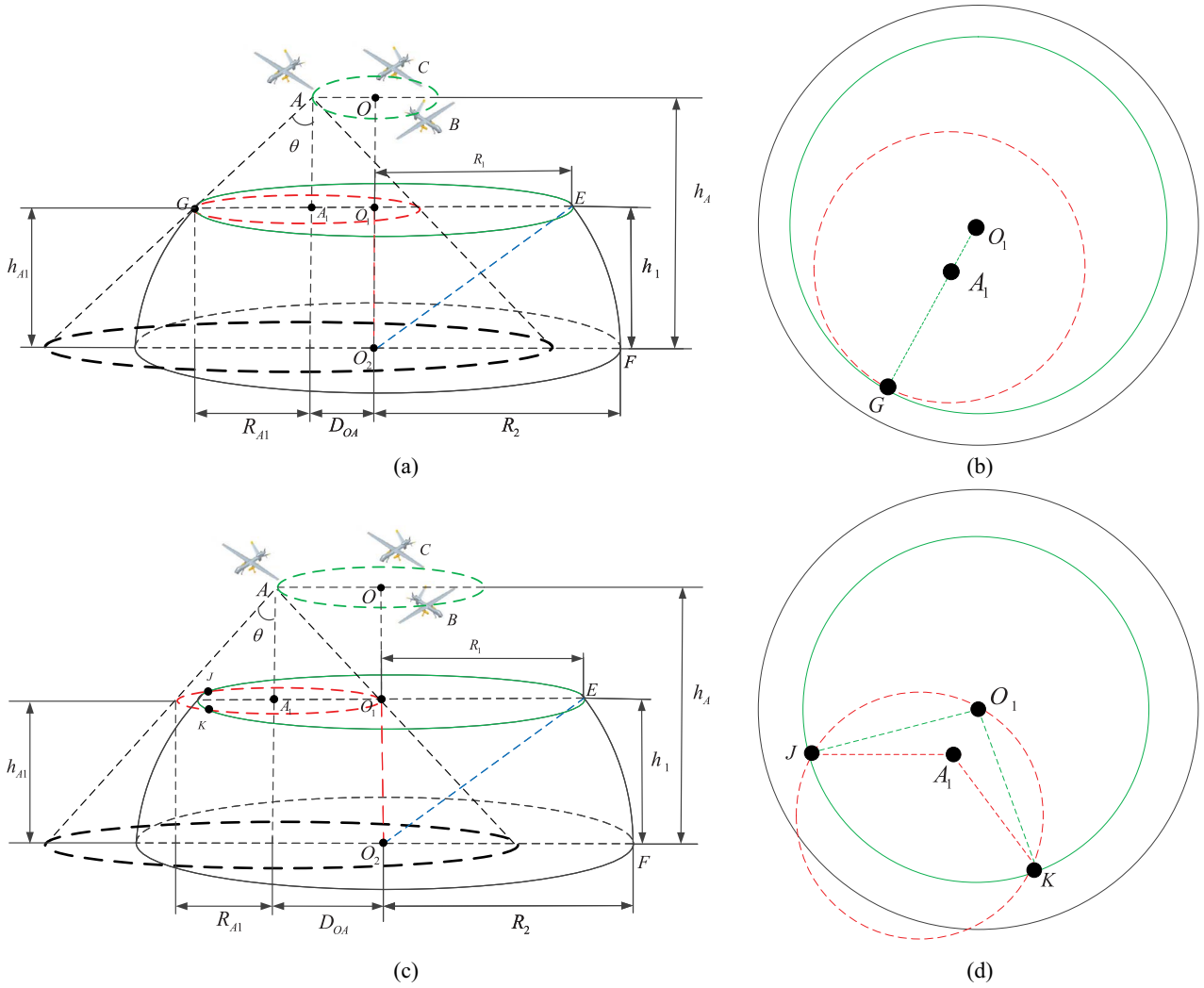

Fig. 6. Geometrical coverage model of upper layer UAVs for case 2. (a) D_{OA} is the minimum from side view. (b) D_{OA} is the minimum from top view. (c) D_{OA} is the maximum from side view. (d) D_{OA} is the maximum from top view.

needed to ensure the communication among lower layer UAVs. Therefore, the LLRA is proposed based on the minimum average transmission delay analyzed in Section IV-B.

A. Equivalent Coverage Blind Zone

To simplify this problem analysis, the coverage of upper layer UAVs is assumed to be equivalent to one virtual UAV in the center of upper layer in Fig. 7(c)–(f), from the side view and the top view, respectively. It is also assumed that there are n_1 upper layer UAVs in Fig. 7(d) and (f), where $n_1 \leq N_{\min}$ and $\angle Y_1 O_1 A_1 = (\pi/n_1)$. The distance between Y and O is depicted by $d_{Y_1 O_1}$ in (17), where $d_{Y_1 A_1}$ represents the distance between Y_1 and A_1, and $d_{O_1 A_1}$ denotes the distance between O_1 and A_1, respectively

$$d_{Y_1 O_1} = \frac{d_{Y_1 A_1} \sin(\angle Y_1 A_1 O_1)}{\sin(\angle Y_1 O_1 A_1)} = \frac{d_{Y_1 A_1} \sin\left(\pi - \arcsin \frac{d_{O_1 A_1} \sin(\angle Y_1 O_1 A_1)}{d_{Y_1 A_1}} - \angle Y_1 O_1 A_1\right)}{\sin(\angle Y_1 O_1 A_1)}. \tag{17}$$

As shown in Fig. 8, Y_1 and Y_2 depict the edge of effective coverage area of UAV A in the top and bottom planes in the lower layer, where their coordinates are calculated by (18) and (19). Therefore, the equivalent height h_4 and the equivalent radiation angle θ_4 are achieved by (20) and (21) in Fig. 8, where

$$C_1 = \arcsin \frac{D_{OA}^{\theta} \sin\left(\frac{\pi}{n_1}\right)}{\left(h_{\max}^{\theta} - h_1\right) \tan(\theta)}$$

$$C_2 = \arcsin \frac{D_{OA}^{\theta} \sin\left(\frac{\pi}{n_1}\right)}{h_{\max}^{\theta} \tan(\theta)}$$

$$Y_1 : \left(0, \frac{\left(h_{\max}^{\theta} - h_1\right) \tan(\theta) \sin(\pi - C_1 - \frac{\pi}{n_1})}{\sin\left(\frac{\pi}{n_1}\right)}, h_1\right) \tag{18}$$

$$Y_2 : \left(0, \frac{h_{\max}^{\theta} \tan(\theta) \sin(\pi - C_2 - \frac{\pi}{n_1})}{\sin\left(\frac{\pi}{n_1}\right)}, 0\right) \tag{19}$$

$$h_4 = \frac{h_1 h_{\max}^{\theta} \tan(\theta)}{h_{\max}^{\theta} \tan(\theta) - \left(h_{\max}^{\theta} - h_1\right) \tan(\theta)} = h_{\max}^{\theta} \tag{20}$$

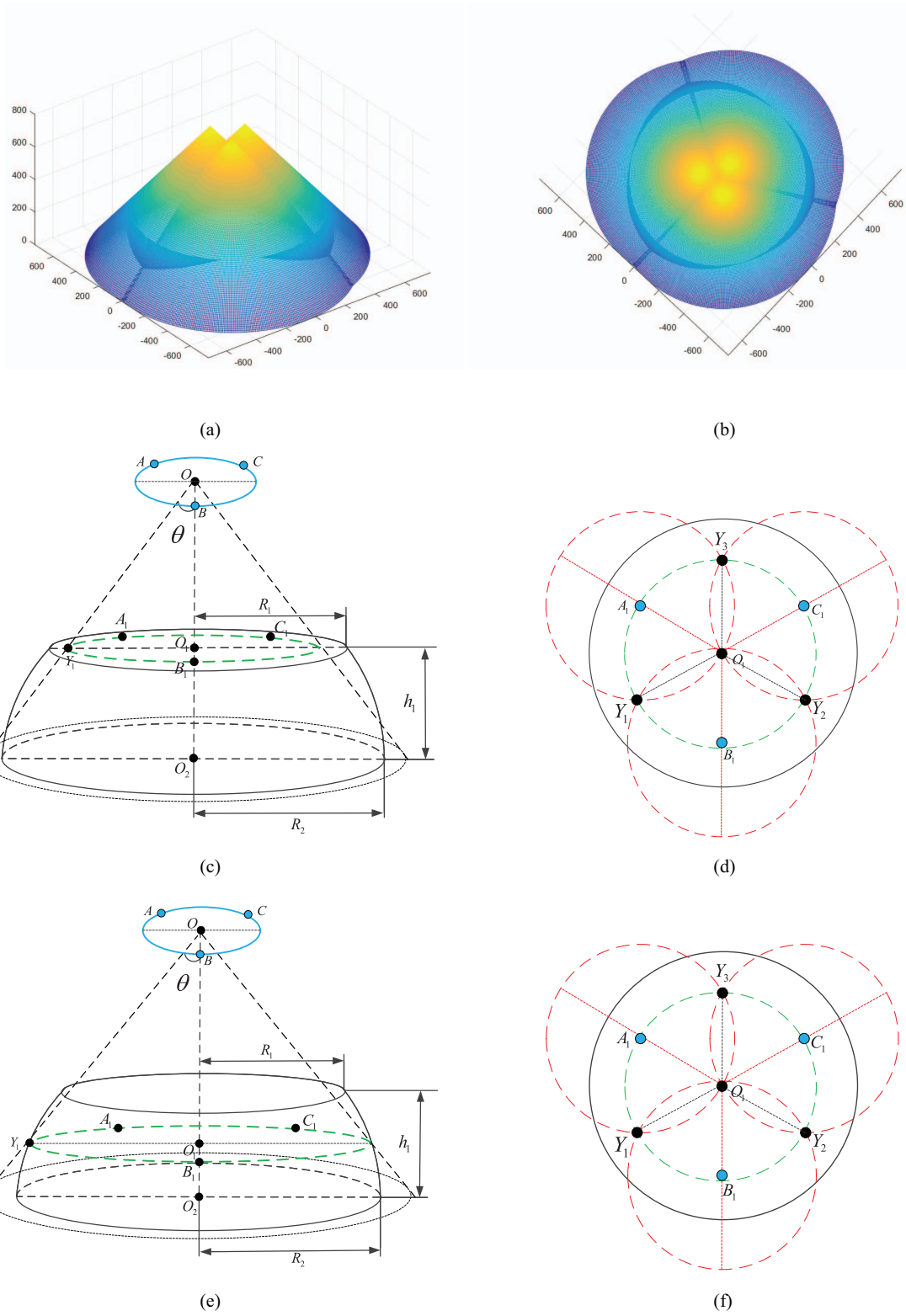

Fig. 7. Equivalent coverage model with coverage blind zones. (a) Volcano-shaped coverage blind zones from side view. (b) Volcano-shaped coverage blind zones from top view. (c) Equivalent coverage of virtual upper layer UAV from side view. (d) Equivalent coverage of virtual upper layer UAV from top view. (e) Equivalent coverage blind zone of virtual upper layer UAV from side view. (f) Equivalent coverage blind zone of virtual upper layer UAV from top view.

$$\theta_4 = \arctan\left(\frac{\tan(\theta)\sin(\pi - \arcsin\frac{D^{\theta}_{OA}\sin\left(\frac{\pi}{n_1}\right)}{h^{\theta}_{\max}\tan(\theta)} - \frac{\pi}{n_1})}{\sin\left(\frac{\pi}{n_1}\right)}\right). \tag{21}$$

Thus, the equivalent coverage zone is defined by $\{x^2 + y^2 \le [(h_4 - z)\tan\theta_4]^2$ and $0 \le z \le h_0\}$. At the same time, the equivalent coverage blind zones are depicted by the rest parts of lower layer, which are outside the equivalent coverage zone.

TABLE I
KEY PARAMETER AND NOTATION IN LLRA

Parameter	Description
N_i	UAV nodes
S	UAV source node
D	UAV destination node
U	Upper layer UAV node
R_i	UAV relay node
S_{N_i}	Direct communication node set of N_i
S_S	Direct communication node set of S
S_D	Direct communication node set of D
S_U	Direct communication node set of U
T_{R_i}	Transmission delay via relay node R_i
A_{R_i}	Relay update area for R_i

B. Average Transmission Delay

Furthermore, the average transmission delay is defined by $D_T(d_{ij})$ in (22) between node i and node j with a distance of d_{ij} based on [24], where T_1 is the packet preparation delay and T_2 is the packet transmission delay. We also assume that the packet transmission is successful when SINR is larger than a predefined threshold β. Thus, the average retransmission time is defined by $\overline{R_{ij}}$ in (23) based on (3)

$$D_T(d_{ij}) = \overline{R_{ij}}(T_1 + T_2) \tag{22}$$

$$\overline{R_{ij}} = \frac{1}{P(\mathrm{SINR}_{ij} \geq \eta)} = \begin{cases} \exp\left(\frac{\eta d_{ij}^{\alpha}(N_0+U_I)}{P_{ij}}\right), & i,j \in \Phi x \\ \exp\left(\frac{\eta d_{ij}^{\alpha}(N_0+U_I)}{g_m P_{ij}}\right), & i \in \Phi s, j \in \Phi x. \end{cases} \tag{23}$$

Based on (22) and (23), the average transmission delay $D_T(d_{ij})$ is given by (24). The total transmission delay is depicted by T_N in (25) after N times of data transmission, where d_{ijk} is the distance between node i and node j at the kth transmission

$$D_T(d_{ij}) = \begin{cases} \exp\left(\frac{\eta {d_{ij}}^{\alpha}(N_0+U_I)}{P_{ij}}\right)(T_1 + T_2), & i,j \in \Phi x \\ \exp\left(\frac{\eta {d_{ij}}^{\alpha}(N_0+U_I)}{g_m P_{ij}}\right)(T_1 + T_2), & i \in \Phi s, j \in \Phi x \end{cases} \tag{24}$$

$$T_N = \sum_{k=1}^{N} D_T(d_{ijk}) = \begin{cases} \sum_{k=1}^{N}\left[\exp\left(\frac{\eta {d_{ijk}}^{\alpha}(N_0+U_I)}{P_{ij}}\right)(T_1 + T_2)\right], & i,j \in \Phi x \\ \sum_{k=1}^{N}\left[\exp\left(\frac{\eta {d_{ijk}}^{\alpha}(N_0+U_I)}{g_m P_{ij}}\right)(T_1 + T_2)\right], & i \in \Phi s, j \in \Phi x. \end{cases} \tag{25}$$

C. Low Latency Routing Algorithm in Layered UAV Network

Based on the analysis of average transmission delay, the LLRA is designed in the proposed layered architecture. Key parameters and notations in LLRA are shown in Table I. To simplify the analysis of the proposed routing algorithm, the following assumptions are considered in this paper.

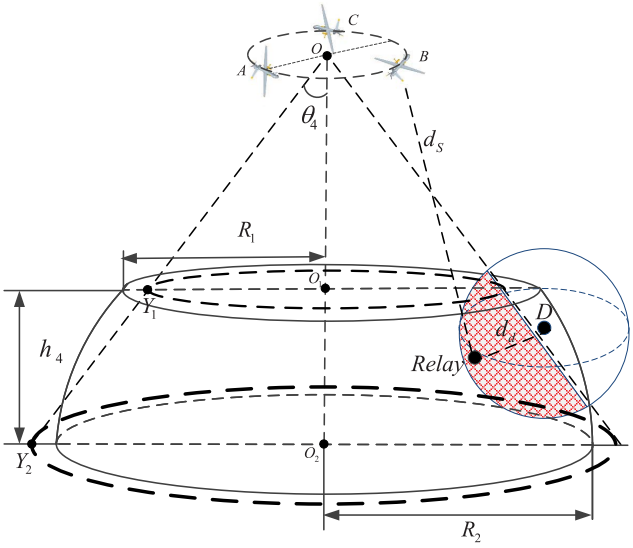

Fig. 8. Equivalent coverage model of upper layer UAVs as relay nodes.

1) To simplify the analysis, we assume that upper layer UAVs are equivalent to one virtual UAV node U at the center of the circular trajectory within the upper layer in Fig. 8.
2) The local information of nearby UAV nodes within one hop is known to all UAVs. Thus, the set of nodes that N_i can communicate directly is defined by S_{N_i}.
3) In terms of the delay caused by multiple hops, at most four hops are considered in the proposed routing algorithm.
4) Upper layer UAV U can communicate with all lower layer UAVs directly based on their location information.
5) Only the UAV within the coverage blind zone cannot communicate directly via upper layer UAVs.

If the source node S cannot communicate with D directly, an initial routing from S to D is established via multiple relay nodes, where the upper layer node U acts as an initial relay node R_i. The initial routing needs to be updated to minimize the transmission delay, and the optimal low latency routing will be established until no relay node could be updated again.

To update the relay node R_a of initial routing $R_{a-1} - R_a - R_{a+1}$ quickly, the relay update area (RUA) is proposed by A_{R_a}. And the transmission delay of the routing $R_{a-1} - R_i - R_{a+1}$ by T_{R_i} should be less than that of the initial routing $R_{a-1} - R_a - R_{a+1}$ by T_{R_a} in (26), where R_i denotes any node in A_{R_a}, $d_{R_{a-1}R_i}$ denotes the distance between node R_{a-1} and node R_i, and $d_{R_iR_{a+1}}$ denotes the distance between node R_i and node R_{a+1}. Therefore, only the nodes in A_{R_a} need to be considered to select the optimal relay node to replace the initial relay node R_a, which will reduce the update time greatly

$$T_{R_i} = D_T(d_{R_{a-1}R_i}) + D_T(d_{R_iR_{a+1}}) \leq T_{R_a}. \tag{26}$$

Based on (24) and (26), the conditions needed to be met by $d_{R_{a-1}R_i}$ and $d_{R_iR_{a+1}}$ for node R_i in A_{R_a} are depicted in (27), where $A = (T_1 + T_2)$, $B_1 = \eta(N_0 + U_I)/P_{ij}$ and $B_2 = \eta(N_0 + U_I)/g_m P_{ij}$. Therefore, the RUA A_{R_a} of relay node R_a in the routing of $R_{a-1} - R_a - R_{a+1}$ is identified based

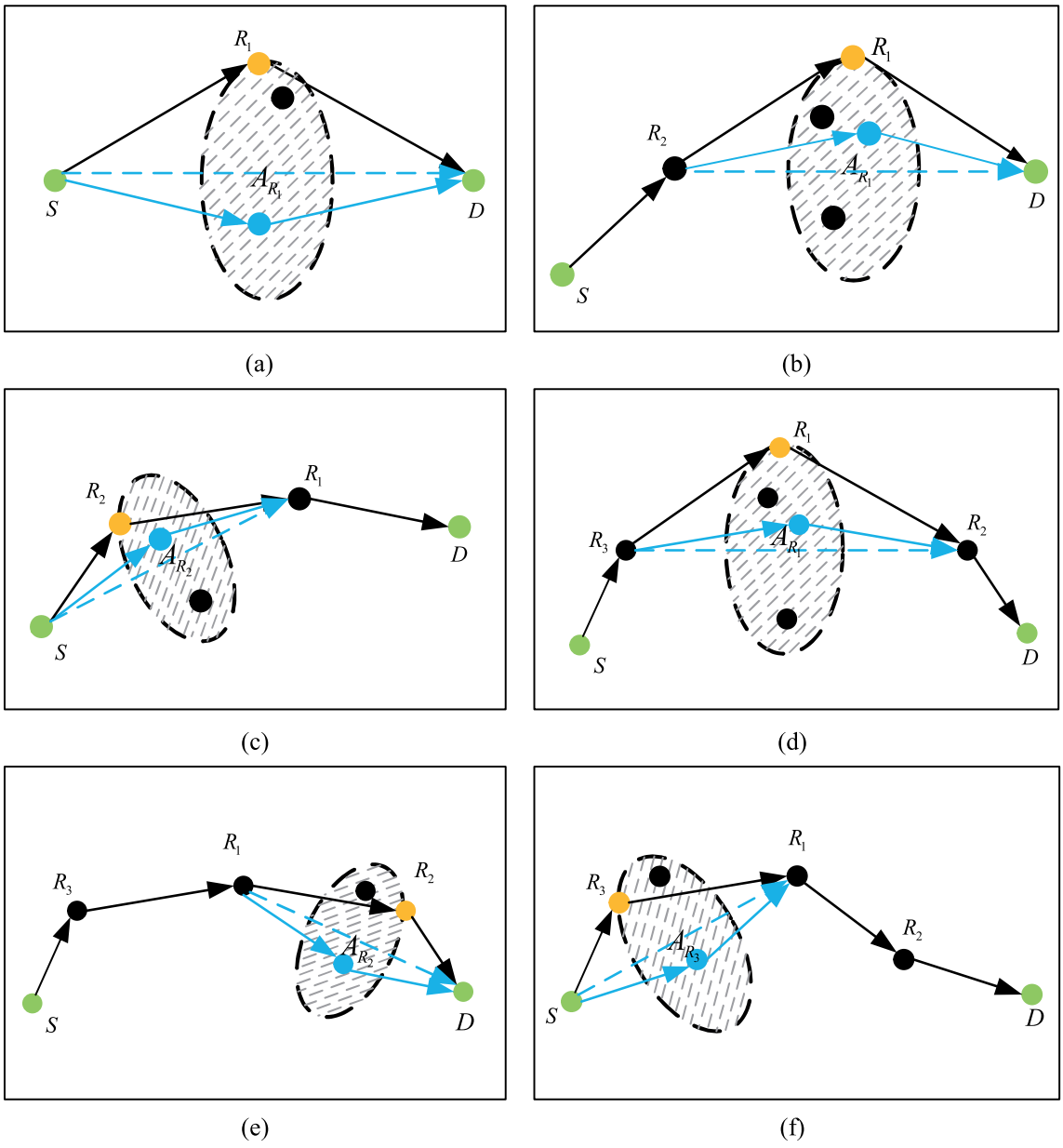

Fig. 9. LLRA. (a) Initial route establishment via one relay node. (b) and (c) Route update via two relay nodes. (d)–(f) Route update via three relay nodes.

on (28) by the shadow area in Fig. 9, where (x_i, y_i, z_i) denotes the position coordinates of node R_i

$$d_{R_{a-1}R_i}{}^{\alpha} + d_{R_iR_{a+1}}{}^{\alpha} \leq \begin{cases} 2\ln\left(\frac{T_{R_a}}{2A}\right)/B_1, R_i \in \Phi x \\ 2\ln\left(\frac{T_{R_a}}{2A}\right)/B_2, R_i \in \Phi s \end{cases} \tag{27}$$

$$A_{R_a} = \left\{(x_i, y_i, z_i) | d_{R_{a-1}R_i}{}^{\alpha} + d_{R_iR_{a+1}}{}^{\alpha} \leq 2\ln\left(\frac{T_{R_a}}{2A}\right)/B\right\}. \tag{28}$$

Therefore, the LLRA is designed in Algorithm 1 as depicted by Fig. 9, which will first establish an initial route in step 1 and update the relay nodes to minimize the transmission delay in step 2. The route update procedure is carried out periodically to guarantee the connectivity and the minimum transmission delay in step 3.

Step 1 (Initial Route Establishment):

1) If the source node S can communicate with D directly, then the route is established as $S - D$.
2) If $D \notin S_S$ and both S and D are not in the coverage blind zone ($S \in S_U, D \in S_U$), the source node S will first communicate with the upper layer node U as the relay node R_1 in order to reach the destination node D, where the initial route is denoted by $S - R_1 - D$ in Fig. 9(a). Accordingly, the optimal routing algorithm is updated by step 2-1.
3) If $D \notin S_S$ and D is in the coverage blind zone ($D \notin S_U$), the source node S will first communicate with the upper layer node U as an initial relay node R_2. Then, another relay node R_1 is chosen from the intersection area

Algorithm 1 LLRA

Input: the source node S and the destination node D.
Output: the optimal low latency route.
Step 1: Initial route establishment.
Establish an initial route based on the relationship between S, D and U.
Step 2: Route update.
Step 2-1: Route update via one relay node.
If $S \in S_D$, the new route is updated as $S - D$.
Calculate Relay Update Area A_{R_1} of R_1.
Select the new relay node R_1 with the minimum transmission delay T_1 in A_{R_1}.
if R_1 has not been updated. **then**
    The route update process ends.
else
    Go to **Step 2-1** again.
end if
Step 2-2: Route update via two relay nodes.
Update the relay node R_1 and R_2 as **Step 2-1** separately.
if None of R_1 and R_2 has been updated. **then**
    The route update process ends.
else
    Go to **Step 2-2** again.
end if
Step 2-3: Route update via three relay nodes.
Update the relay node R_1, R_2 and R_3 as **Step 2-1** separately.
if None of R_1, R_2 and R_3 has been updated. **then**
    The route update process ends.
else
    Go to **Step 2-3** again.
end if
Step 3: The relay nodes update procedure will be carried out periodically.

between S_U and S_D randomly in order to reach D. Therefore, the initial route is established as $S - R_1 - R_2 - D$ in Fig. 9(b) and (c), and the optimal routing algorithm is updated by step 2-2.

4) If $D \notin S_S$ and S is in the coverage blind zone ($S \notin S_U$), the source node S will first communicate with R_2 which is chosen from the intersection area between S_S and S_U randomly, to reach the upper layer UAV node U which acts as the initial relay node R_1. The initial route is established as $S - R_2 - R_1 - D$ in Fig. 9(b) and (c), and the optimal routing algorithm is updated by step 2-2.
5) If $D \notin S_S$ and both S and D are in the coverage blind zone ($S \notin S_U, D \notin S_U$), the source node S will first communicate with R_3 which is chosen from S_U randomly. The upper layer UAV node U will acts as an initial relay node R_1 to find another relay R_2 from the intersection area between S_U and S_D. The initial route is $S - R_3 - R_1 - R_2 - D$ in Fig. 9(d)–(f), and the optimal routing algorithm is updated by step 2-3.

Step 2 (Route Update): The route update process is divided into three steps based on the number of relay nodes in step 2-1, step 2-2, and step 2-3.

Step 2-1 (Route Update via One Relay Node):

1) If the source node S can communicate with the destination node D directly, the new route is updated as $S - D$.
2) The RUA A_{R_1} of an initial relay node R_1 is calculated by the upper layer node U in Fig. 9(a).
3) The optimal relay node R_1 is updated with the minimum delay T_1 in A_{R_1} by the upper layer node U in Fig. 9(a).
4) If R_1 has not been updated, the existing route is the optimal scheme. Otherwise, turn to step 2-1.

Step 2-2 (Route Update via Two Relay Nodes):

1) To update R_1, if the relay node R_2 can communicate with the destination node D directly, the new route is updated as $S - R_2 - D$. Then, the optimal routing algorithm is simplified to update R_1 in Fig. 9(a) by step 2-1. Otherwise, the optimal relay node R_1 is updated with the minimum transmission delay T_1 in A_{R_1} by the upper layer node U in Fig. 9(b).
2) Then, update R_2 by using the procedure of step 2-2 1) as denoted by Fig. 9(c).
3) If none of R_1 and R_2 has been updated, the existing route is the optimal scheme. Otherwise, turn to step 2-2.

Step 2-3 (Route Update via Three Relay Nodes):

1) To update R_1, if R_3 can communicate with R_2 directly, the new route is updated as $S - R_3 - R_2 - D$. Then, the optimal routing algorithm is simplified to update R_2 and R_3 by step 2-2 in Fig. 9(b) and (c). Otherwise, the optimal relay node R_1 is updated with the minimum delay T_1 in A_{R_1} by the upper layer node U, as shown in Fig. 9(d).
2) Update R_2 as step 2-3 1) in Fig. 9(e).
3) Update R_3 as step 2-3 1) in Fig. 9(f).
4) If none of R_1–R_3 has been updated, the existing route is the optimal scheme. Otherwise, turn to step 2-3.

Step 3 (Relay Nodes Periodical Update): The route nodes update procedure will be carried out periodically to ensure the connectivity and the minimum transmission delay requirements.

V. Numerical Results

To evaluate the performance of the proposed LLRA routing algorithm in a layered UAV network architecture, the key performance parameters are analyzed and compared to traditional routing algorithms based on simulation results, in terms of the link average delay and the packet delivery ratio.

A. Simulation Setup

As shown in Table II, the layered UAV network is considered in the simulation scenario, where $R_1 = 600$ m, $R_2 = 300\sqrt{3}$ m, and $h_1 = 300$ m. There are 200–300 UAVs with a speed of 0–30 m/s in the lower layer. Based on the theoretical analysis result in Section III, there are $N_{\min} = 3$ UAVs with a maximum flight height h_u that fly around a circle at a speed of 80 m/s in the upper layer. The transmission power of UAV is defined by $P_{ij} = 20$ dBm, and the mean path-loss exponent is $\alpha = 4$. The SINR threshold for a successful transmission among UAVs is defined by $\eta = 0$ dB. The packet

TABLE II
SIMULATION PARAMETERS FOR LAYERED UAVS NETWORK

Parameter	Description
System bandwidth	10 MHz
Radiation angle range of directional antenna θ	$15^o - 60^o$
Transmit power	30 dBm
Range of lower layer	$R_1 = 600$ m, $R_2 = 300\sqrt{3}$ m, $h_1 = 300$ m
Number of lower layer UAVs	200-300
Speed of lower layer UAVs	0-30 m/s
Flight height of upper layer UAVs h_u	800 m
Minimum number of upper layer UAVs	3
Speed of upper layer UAVs	80 m/s
Path loss exponent α	4
SINR threshold η	0 dB
Packet preparation delay T_1	0 us
Packet transmission delay T_2	50 us

preparation delay is $T_1 = 0$ us and the packet transmission delay is $T_2 = 50$ us in [25].

B. Optimal Layered UAV Network Design

The maximum effective coverage time ratio $t_{\max}$ can be achieved with the radiation angles θ based on (11) and (16), and the range of radiation angle of upper layer UAVs is $[\theta_{\min}, \theta_{\max}]$, where $\theta_{\min} = 15°$ and $\theta_{\max} = 60°$ in Fig. 10. However, considering the constrained limitations between the flying altitude and radiation angle of the upper UAV, not all radiation angle are effective.

The effective radiation angle of UAVs in the upper layer with various altitude limits is shown in Fig. 10 in two typical cases divided by the dotted line based on theoretical analysis results in Section III. The maximum flight altitude h_u of upper layer UAVs is depicted by the blue line of 800 m. The green line stands for the minimum height of the upper layer UAV which can cover the whole lower layer by itself as depicted by $(R_2/\sin\theta)$ and $h_1 + (R_1/\tan\theta)$, when $\theta_{\min} = 15° \le \theta \le 30° = \angle EO_2F$ and $\angle EO_2F = 30° \le \theta \le 60° = \theta_{\max}$, respectively. Moreover, the maximum height of UAV limited by its communication capability of $\mathrm{d}_{\max}\cos\theta$ is depicted by the red line. The black line is the minimum height of upper layer UAVs which can achieve a full coverage for the lower layer cooperatively as $[(h_1\cos^2\theta)/(2\sin^2\theta)] + R_2\sin\theta$ and $h_1 + (R_1/2\tan\theta)$, when $\theta_{\min} = 15° \le \theta \le 30° = \angle EO_2F$ and $\angle EO_2F = 30° \le \theta \le 60° = \theta_{\max}$, respectively.

Constrained by these parameters, the effective radiation angle of UAVs ranges from 28.36° to 60° as shown by the shadow area in Fig. 10. Therefore, the maximum altitude $h^{\theta}_{\max}$ = 800 m when $28.36° \le \theta \le 37.35°$ and $h^{\theta}_{\max} = d_{\max}\cos\theta$, when $37.35° \le \theta \le 60°$.

Therefore, the maximum effective coverage time ratio $t_{\max}$ with different radiation angles θ is shown in Fig. 11 based on (11) and (16). From Fig. 11 we can see that, the maximum effective coverage time ratio increases as the radiation angle θ increases from 28.36° to 48.08°. When $48.08° \le \theta \le 60°$, the maximum coverage ratio t will decrease as the radiation angle θ increases. Therefore, the maximum effective coverage

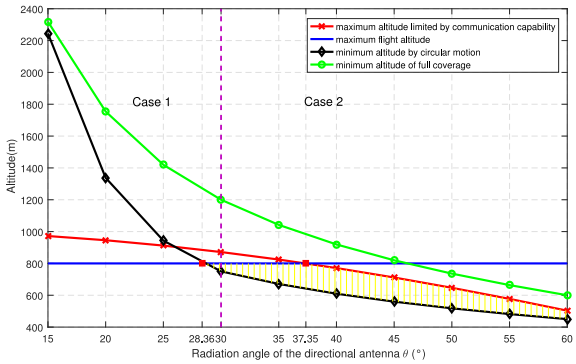

Fig. 10. Effective radiation angle with various altitude limits.

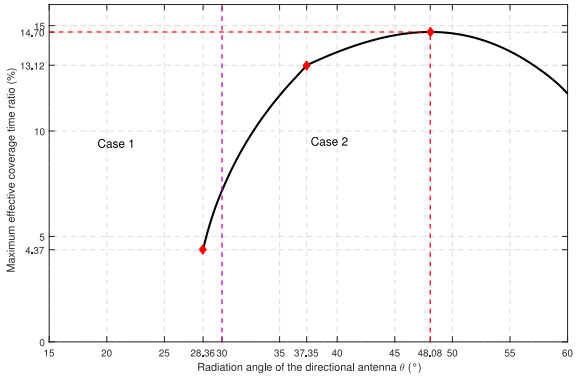

Fig. 11. Maximum effective coverage time ratio with different radiation angles.

time ratio $t_{\max}$ is achieved by 14.7% when $\theta = 48.08°$, and the optimal position of UAV in the upper layer is $h^{\theta}_{\max}$ = 672.31 m, where D^{θ}_{OA} = 313.33 m. Finally, the layered UAV network architecture design problem as proposed in Section III has been solved with proof results in Fig. 11.

C. Performance of LLRA

To verify the performance of the proposed LLRA in a layered UAV network architecture, both link average delay and

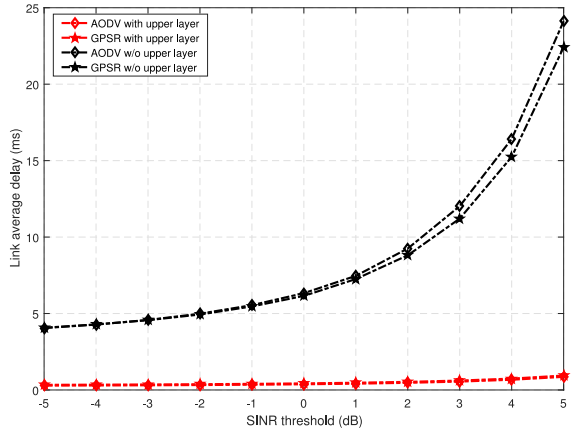

Fig. 12. Link average delay comparison with or w/o upper layer UAVs.

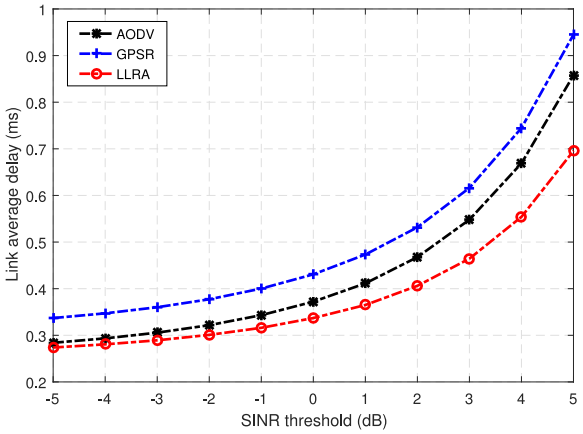

Fig. 14. Link average delay of different routing algorithms.

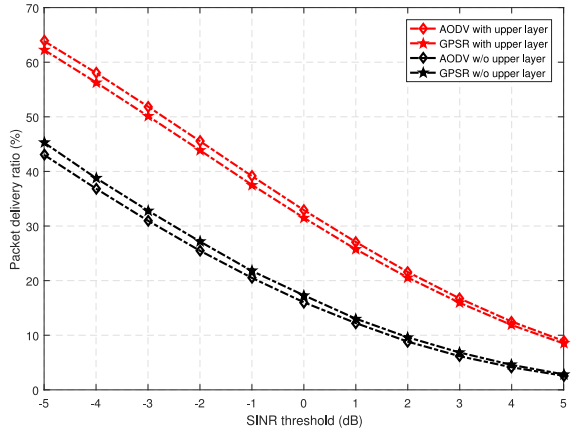

Fig. 13. Packet delivery ratio comparison with or w/o upper layer UAVs.

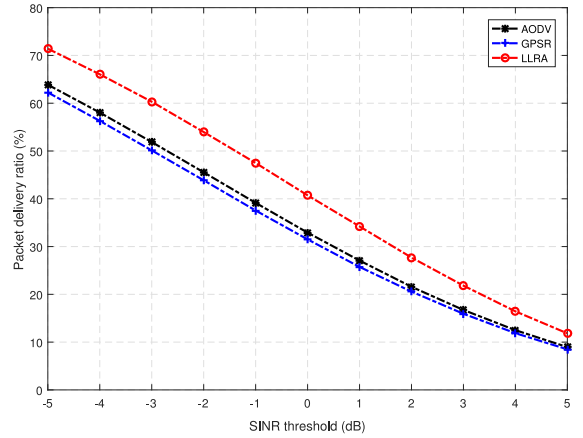

Fig. 15. Packet delivery ratio of different routing algorithms.

packet delivery ratio are considered as key parameters by comparing the results with traditional AODV and GPSR algorithms. In Fig. 12, the link average delay of traditional AODV and GPSR routing algorithms with upper layer relay nodes is lower than that without the upper layer nodes. Similarly, as shown in Fig. 13, the packet delivery ratio of AODV and GPSR routing algorithms with the upper layer relay nodes is higher than that without the upper layer nodes. Because the number of hops under different routing paths generated by AODV and GPSR routing algorithms with upper layer relay nodes is less than that without the upper layer nodes, the decrease of hops will increase the probability of successful packet transmission, leading to the drop of delay and the increase of successful packet delivery ratio. Therefore, the performances of traditional AODV and GPSR routing algorithms are improved by using layered UAV network architecture, which proves the effectiveness of the proposed network architecture.

Furthermore, both link average delay and packet delivery ratio of the proposed LLRA algorithm are verified in Figs. 14 and 15, in contrast to traditional AODV and GPSR routing algorithms. In Fig. 14, the link average delay of these routing algorithms increases as SINR threshold increases. But, the packet delivery ratio decreases as SINR threshold increases. With the increase of SINR threshold, the amount of received information will grow accordingly. However, the growth of noise and interference is much bigger than the information increase, leading to the decrease of successful packet transmission and the increase of delay. Besides, the average delay ratio of the proposed LLRA algorithm is much lower than that of AODV and GPSR algorithms, and the packet delivery ratio of LLRA algorithm is higher than that of AODV and GPSR algorithms in Figs. 14 and 15. Because the route of the proposed LLRA algorithm contains upper layer UAVs as relay nodes, the hops of LLRA algorithm are less than that of AODV and GPSR algorithms, leading to the decrease of delay and the increase of packet delivery ratio. Therefore, the proposed LLRA algorithm performs better than AODV and GPSR algorithms in both link average delay and packet delivery ratio, which can achieve the optimal design of LLRA algorithm.

VI. Conclusion

In this paper, a layered UAV network architecture has been proposed and the minimum number of upper layer UAVs is theoretically proved by closed-form coverage boundaries. Based on the proposed layered network architecture, the LLRA has been designed based on the partial location information and the connectivity of upper layer UAVs. Numerical results prove that the proposed LLRA algorithm performs better than

the traditional AODV and GPSR algorithms in terms of the link average delay and the packet delivery ratio.

In our future research work, we will consider the machine learning-based UAV network optimization in terms of the routing algorithms, and intelligence enabled UAV communication technologies. To be specific, we will focus on the machine learning-based target detection and mobility prediction for UAV platform, communication and computation fusion enabled low latency transmission in UAVs swarm network, and prototype the sensing and communication converged system for V2V and UAV scenarios.

REFERENCES

[1] L. Gupta, R. Jain, and G. Vaszkun, "Survey of important issues in UAV communication networks," *IEEE Commun. Surveys Tuts.*, vol. 18, no. 2, pp. 1123–1152, 2nd Quart., 2016.

[2] S. Hayat, E. Yanmaz, and R. Muzaffar, "Survey on unmanned aerial vehicle networks for civil applications: A communications viewpoint," *IEEE Commun. Surveys Tuts.*, vol. 18, no. 4, pp. 2624–2661, 4th Quart., 2016.

[3] A. Al-Hourani, S. Kandeepan, and A. Jamalipour, "Modeling air-to-ground path loss for low altitude platforms in urban environment," in *Proc. IEEE GLOBECOM*, Austin, TX, USA, Dec. 2014, pp. 2898–2904.

[4] I. Bor-Yaliniz and H. Yanikomeroglu, "The new Frontier in RAN heterogeneity: Multi-tier drone-cells," *IEEE Commun. Mag.*, vol. 54, no. 11, pp. 48–55, Nov. 2016.

[5] F. Cheng, S. Zhang, Z. Li, and Y. Chen, "UAV trajectory optimization for data offloading at the edge of multiple cells," *IEEE Trans. Veh. Technol.*, vol. 67, no. 7, pp. 6732–6736, Jul. 2018.

[6] N. Zhao *et al.*, "Caching UAV assisted secure transmission in hyper-dense networks based on interference alignment," *IEEE Trans. Commun.*, vol. 66, no. 5, pp. 2281–2294, May 2018.

[7] C. Zhang and W. Zhang, "Spectrum sharing for drone networks," *IEEE J. Sel. Areas Commun.*, vol. 35, no. 1, pp. 136–144, Jan. 2017.

[8] N. H. Motlagh, T. Taleb, and O. Arouk, "Low-altitude unmanned aerial vehicles-based Internet of Things services: Comprehensive survey and future perspectives," *IEEE Internet Things J.*, vol. 3, no. 6, pp. 899–922, Dec. 2016.

[9] Y. Zhou, N. Cheng, N. Lu, and X. S. Shen, "Multi-UAV-aided networks: Aerial-ground cooperative vehicular networking architecture," *IEEE Veh. Technol. Mag.*, vol. 10, no. 4, pp. 36–44, Dec. 2015.

[10] A. Al-Hourani, S. Kandeepan, and S. Lardner, "Optimal LAP altitude for maximum coverage," *IEEE Wireless Commun. Lett.*, vol. 3, no. 6, pp. 569–572, Dec. 2014.

[11] M. Alzenad, A. El-Keyi, F. Lagum, and H. Yanikomeroglu, "3-D placement of an unmanned aerial vehicle base station (UAV-BS) for energy-efficient maximal coverage," *IEEE Wireless Commun. Lett.*, vol. 6, no. 4, pp. 434–437, Aug. 2017.

[12] M. Mozaffari, W. Saad, M. Bennis, and M. Debbah, "Drone small cells in the clouds: Design, deployment and performance analysis," in *Proc. IEEE GLOBECOM*, San Diego, CA, USA, Dec. 2015, pp. 1–6.

[13] S. Koulali, E. Sabir, T. Taleb, and M. Azizi, "A green strategic activity scheduling for UAV networks: A sub-modular game perspective," *IEEE Commun. Mag.*, vol. 54, no. 5, pp. 58–64, May 2016.

[14] M. Mozaffari, W. Saad, M. Bennis, and M. Debbah, "Optimal transport theory for power-efficient deployment of unmanned aerial vehicles," in *Proc. IEEE ICC*, Kuala Lumpur, Malaysia, May 2016, pp. 1–6.

[15] G. Gankhuyag, A. P. Shrestha, and S. J. Yoo, "Robust and reliable predictive routing strategy for flying ad-hoc networks," *IEEE Access*, vol. 5, pp. 643–654, 2017.

[16] J. Jiang and G. Han, "Routing protocols for unmanned aerial vehicles," *IEEE Commun. Mag.*, vol. 56, no. 1, pp. 58–63, Jan. 2018.

[17] C.-M. Cheng, P.-H. Hsiao, H. T. Kung, and D. Vlah, "Maximizing throughput of UAV-relaying networks with the load-carry-and-deliver paradigm," in *Proc. IEEE WCNC*, Kowloon, China, Mar. 2007, pp. 4417–4424.

[18] Y. Zheng *et al.*, "A mobility and Load aware OLSR routing protocol for UAV mobile ad-hoc networks," in *Proc. Int. Conf. Inf. Commun. Technol. (ICT)*, Nanjing, China, May 2014, pp. 1–7.

[19] S. Rosati, K. Kruzelecki, L. Traynard, and B. R. Mobile, "Speed-aware routing for UAV ad-hoc networks," in *Proc. IEEE GLOBECOM Workshops*, Atlanta, GA, USA, Dec. 2013, pp. 1367–1373.

[20] H. Simaremare, A. Syarif, A. Abouaissa, R. F. Sari, and P. Lorenz, "Performance comparison of modified AODV in reference point group mobility and random waypoint mobility models," in *Proc. IEEE ICC*, Budapest, Hungary, Jun. 2013, pp. 3542–3546.

[21] J.-D. M. M. Biomo, T. Kunz, and M. St-Hilaire, "Routing in unmanned aerial ad hoc networks: Introducing a route reliability criterion," in *Proc. 7th IFIP Wireless Mobile Netw. Conf. (WMNC)*, Vilamoura, Portugal, May 2014, pp. 1–7.

[22] S. Funke and N. Milosavljevic, "Guaranteed-delivery geographic routing under uncertain node locations," in *Proc. INFOCOM*, Barcelona, Spain, May 2007, pp. 1244–1252.

[23] M. T. Hyland, B. E. Mullins, R. O. Baldwin, and M. A. Temple, "Simulation-based performance evaluation of mobile ad hoc routing protocols in a swarm of unmanned aerial vehicles," in *Proc. 21st Int. Conf. Adv. Inf. Netw. Appl. Workshops (AINAW)*, vol. 2. Niagara Falls, ON, Canada, May 2007, pp. 249–256.

[24] D. Hu, J. Wu, and P. Fan, "Minimizing end-to-end delays in linear multihop networks," *IEEE Trans. Veh. Technol.*, vol. 65, no. 8, pp. 6487–6496, Aug. 2016.

[25] Y. Xiao and L. J. Cimini, "Spectral efficiency of distributed cooperative relaying," in *Proc. 45th Annu. Conf. Inf. Sci. Syst.*, Baltimore, MD, USA, Mar. 2011, pp. 1–6.

[26] S. Srinivasa and M. Haenggi, "Distance distributions in finite uniformly random networks: Theory and applications," *IEEE Trans. Veh. Technol.*, vol. 59, no. 2, pp. 940–949, Feb. 2010.

Qixun Zhang (M'12) received the B.S. and Ph.D. degrees from the Beijing University of Posts and Telecommunications (BUPT), Beijing, China, in 2006 and 2011, respectively.

He is an Associate Professor with the Key Laboratory of Universal Wireless Communications, Ministry of Education, BUPT. In 2006, he was a Visiting Scholar with the University of Maryland at College Park, College Park, MD, USA, for three months. He is currently a Visiting Scholar with the Electrical and Computer Engineering Department, University of Houston, Houston, TX, USA. His current research interests include fifth generation mobile networks, cognitive radio and heterogeneous networks, game theory, LAA and LTE-U systems, sensing and communication integrated system design, and unmanned aerial vehicles communication.

Dr. Zhang is an active with ITU-R WP5A/5C/5D, IEEE 1900, CCSA, and IMT-2020(5G) standards.

Menglei Jiang (S'18) is currently pursuing the master's degree at the School of Information and Communication Engineering, Beijing University of Posts and Telecommunications, Beijing, China.

His current research interests include unmanned aerial vehicles communication, vehicular networks, and unmanned aerial vehicles routing algorithms.

Zhiyong Feng (M'08–SM'15) received the B.S., M.S., and Ph.D. degrees from the Beijing University of Posts and Telecommunications (BUPT), Beijing, China.

She is a Professor and the Director of the Key Laboratory of Universal Wireless Communications, Ministry of Education, BUPT. Her current research interests include wireless network architecture design and radio resource management in fifth generation mobile networks, spectrum sensing and dynamic spectrum management in cognitive wireless networks, universal signal detection and identification, and network information theory.

Dr. Feng is an active in standards development, such as ITU-R WP5A/5C/5D, IEEE 1900, ETSI, and CCSA.

Wei Li (M'99–SM'16) received the Ph.D. degree in electrical and computer engineering from the University of Victoria, Victoria, BC, Canada, in 2004.

He is currently an Assistant Professor with Northern Illinois University, DeKalb, IL, USA. His current research interests include computer networks, Internet of Things, e-health, machine learning, and artificial intelligence.

Wei Zhang (F'15) is a Professor with the University of New South Wales, Sydney, NSW, Australia. His current research interests include UAV communications, mmWave communications, space information networks, and massive MIMO.

Mr. Zhang currently serves as a TPC Co-Chair of IEEE/CIC ICCC 2019, Changchun, China. He is the Editor-in-Chief of IEEE WIRELESS COMMUNICATIONS LETTERS and an Associate Editor-in-Chief of the *Journal of Communications and Information Networks*. He also serves as Chair for the IEEE Wireless Communications Technical Committee and the Vice Director of the IEEE Communications Society Asia–Pacific Board. He is a member of the Board of Governors of the IEEE Communications Society.

Miao Pan (S'07–M'12–SM'18) received the B.Sc. degree in electrical engineering from the Dalian University of Technology, Dalian, China, in 2004, the M.A.Sc. degree in electrical and computer engineering from the Beijing University of Posts and Telecommunications, Beijing, China, in 2007, and the Ph.D. degree in electrical and computer engineering from the University of Florida, Gainesville, FL, USA, in 2012.

He is currently an Assistant Professor with the Department of Electrical and Computer Engineering, University of Houston, Houston, TX, USA. His current research interests include big data privacy, cybersecurity, cyber-physical systems, and cognitive radio networking.

Dr. Pan was a recipient of the NSF CAREER Award in 2014 and the Best Paper Award of VTC 2018, Globecom 2017, and Globecom 2015. He was an Associate Editor for the IEEE INTERNET OF THINGS JOURNAL from 2015 to 2018. He is a member of the ACM.